Title: Report on waterproofing of UN studies

Author(s): Shivprasad, Aditya Prahlad
Telles, Amber Celeste
White, Joshua Taylor

Intended for: Report

Issued: 2019-09-11 (rev.1)

APPENDIX E

NTRD DOCUMENT COVER SHEET [1]

Name/Title of Deliverable/Milestone/Revision No. M2FT-19LA020201021 ;Report on waterproofing UN studies

Work Package Title and Number FT-19LA02020102; Advanced Ceramic Fuel Development

Work Package WBS Number 1.02.02.02.01; LWR Fuels

Responsible Work Package Manager _____
(Name/Signature)

Date Submitted 08/22/2019

Quality Rigor Level for Deliverable/Milestone[2]	☐ QRL-1 ☐ Nuclear Data	☐ QRL-2	☒ QRL-3	☐ QRL 4 Lab QA Program[3]

This deliverable was prepared in accordance with Los Alamos National Laboratory
(Participant/National Laboratory Name)

QA program which meets the requirements of
☒ DOE Order 414.1 ☐ NQA-1 ☐ Other

This Deliverable was subjected to:

☒ Technical Review ☐ Peer Review

Technical Review (TR)
Review Documentation Provided
☐ Signed TR Report or,
☐ Signed TR Concurrence Sheet or,
☒ Signature of TR Reviewer(s) below
Name and Signature of Reviewers

Peer Review (PR)
Review Documentation Provided
☐ Signed PR Report or,
☐ Signed PR Concurrence Sheet or,
☐ Signature of PR Reviewer(s) below
Name and Signature of Reviewers

NOTE 1: *Appendix E should be filled out and submitted with each deliverable. Or, if the PICS: NE system permits, completely enter all applicable information in the PICS: NE Deliverable Form. The requirement is to ensure that all applicable information is entered either in the PICS: NE system or by using the NTRD Document Cover Sheet.*

- *In some cases there may be a milestone where an item is being fabricated, maintenance is being performed on a facility, or a document is being issued through a formal document control process where it specifically calls out a formal review of the document. In these cases, documentation (e.g., inspection report, maintenance request, work planning package documentation or the documented review of the issued document through the document control process) of the completion of the activity, along with the Document Cover Sheet, is sufficient to demonstrate achieving the milestone.*

NOTE 2: *If QRL 1, 2, or 3 is not assigned, then the QRL 4 box must be checked, and the work is understood to be performed using laboratory QA requirements. This includes any deliverable developed in conformance with the respective National Laboratory / Participant, DOE or NNSA-approved QA Program.*

NOTE 3: *If the lab has an NQA-1 program and the work to be conducted requires an NQA-1 program, then the QRL-1 box must be checked in the work Package and on the Appendix E cover sheet and the work must be performed in accordance with the Lab's NQA-1 program. The QRL-4 box should not be checked.*

Report on waterproofing of UN studies

Nuclear Technology Research and Development

Prepared for
U.S. Department of Energy
FCRD Program
Aditya P. Shivprasad
Amber C. Telles
Joshua T. White
Los Alamos National Laboratory

August 22, 2019
NTRD-M2FT-19LA020201021
LA-UR-19-28422

SUMMARY

Fuels with high uranium densities have been considered in the Nuclear Technology Research and Development program's Advanced Fuels Campaign as potential replacements for uranium(IV) oxide in commercial light water reactors. One such candidate fuel is uranium mononitride, UN, which has been observed to readily oxidize in steam and simulated pressurized water reactor conditions. Thus, it is important to examine methods for waterproofing UN, especially for potential cladding breach scenarios. This can be achieved by controlling the microstructure so as to prevent contact between the UN fuel and coolant.

Research highlighted in this L2 milestone has focused on screening potential candidate additive materials to control UN microstructure using steam oxidation TGA. From these candidates, silicon (Si), chromium (Cr), and silicon carbide (SiC) were selected based on corrosion resistance, which led to attempts to develop a method for compositing these materials with UN. Powders of these materials were mixed with UN, pressed, and sintered. UN-metal composite sintering was attempted through liquid-phase sintering at temperatures above the melting point of the respective metals, while the UN-SiC composite sintering was attempted using two-step sintering at 2100 and 2050 °C. Results of silicon and silicon carbide appeared to show chemical interaction with UN to form uranium silicides, while chromium was found to significantly volatilize near the melting point of chromium. No indication of densification was observed. These observations, along with those of the preceding, related L3 milestone (NTRD-M3FT-19LA020201024) were used to develop a better understanding of microstructure control to advance efforts for UN waterproofing.

CONTENTS

FIGURES

TABLES

ACRONYMS

LWR	Light water reactor
PWR	Pressurized water reactor
FRL	Fuels Research Laboratory
XRD	X-ray diffraction
TGA	Thermogravimetric analysis/analyzer
PDF	Powder diffraction file

REPORT ON WATERPROOFING OF UN STUDIES

1. INTRODUCTION

Uranium mononitride, UN, is a promising candidate for accident tolerant fuels because of its high thermal conductivity and uranium density, as compared with uranium(IV) oxide (UO_2). Higher thermal conductivity results in lower fuel centerline temperatures during operation and, thus, lower stored energy of the reactor core. High uranium density results in an increased fission density and, thus, allows for a greater neutronic penalty from accident tolerant fuel claddings. Proposed accident tolerant claddings include stainless steel, Fe-Cr-Al (and derivative alloys), and silicon carbide because of their improved resistance to waterside corrosion compared to zirconium-based fuel cladding. However, all of these cladding concepts use elements with higher neutron absorption cross-sections than zirconium. As a result, the improved fission density of uranium mononitride enables the use of these types of cladding in reactors. In addition to accident tolerance with respect to neutronics and thermal conductivity, it is important to assess the behavior of uranium mononitride in a cladding breach scenario. However, resistance of uranium mononitride to waterside corrosion during such conditions has been shown to be poor. In particular, uranium mononitride exposed to high-temperature steam and simulated pressurized water reactor (PWR) environments has been observed to degrade by rapid pulverization.

Previous work in FY18 within the campaign examined the performance of uranium mononitride in a variety of environments such as steam and high-temperature/pressure water with hydrogen water chemistry [1]. Steam tests were carried out *in-situ* using thermogravimetric analysis, while simulated PWR conditions were performed in an autoclave. Work within the campaign also examined the feasibility of waterproofing uranium mononitride by co-sintering with uranium(IV) oxide. Composites of UN/UO_2 were examined for waterside corrosion resistance, as well, showing decreased resistance with increasing uranium mononitride content, given the known resistance of UO_2 to waterside corrosion. Thermogravimetric analysis of UN/UO_2 composites in 62 - 83% steam (varies as a function of temperature for a specific water flowrate) under a temperature ramp to 1000 °C, as evaluated in FY17 work, is shown in Figure 1 for various uranium mononitride contents. Similar data for isotherms at 350 °C and 82% steam is shown in Figure 2. During isothermal waterside corrosion, mass gain and pulverization occurred over the course of minutes, though the addition of uranium(IV) oxide significantly delayed the onset of oxidation. Similarly, during temperature ramps in steam, the addition of UO_2 appeared to delay the onset of oxidation, though pulverization occurred for pellets containing more than 10 volume percent uranium mononitride. Based on these results, it is clear that additions of uranium(IV) oxide are not sufficient to waterproof uranium mononitride. These results drive the need for other methods of waterproofing uranium mononitride using a controlled microstructure.

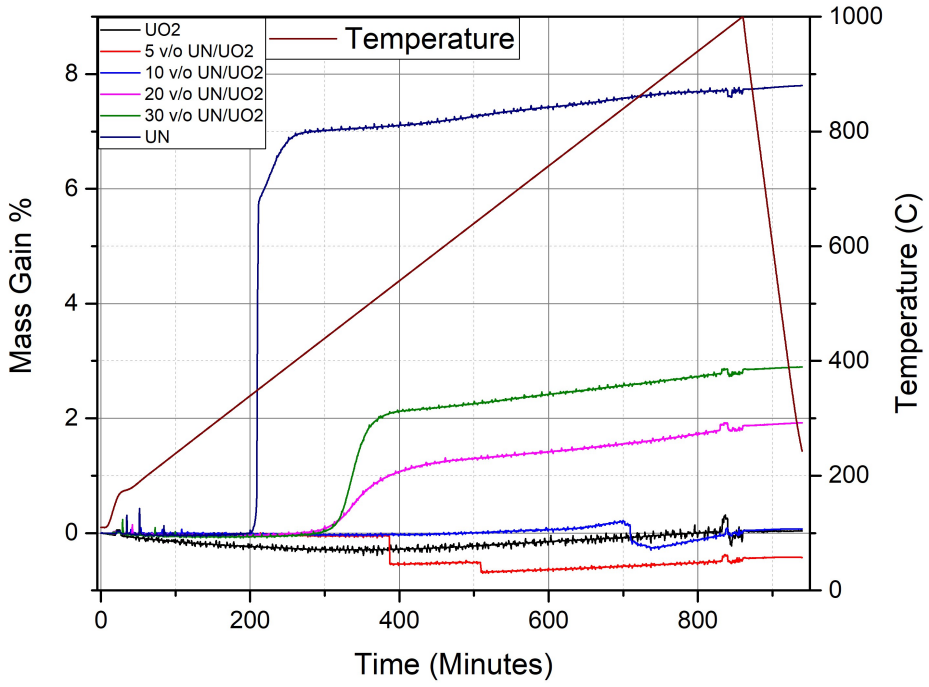

Figure 1: Thermograms comparing mass gain of composite materials (UN/UO_2) and monolithic UN and UO_2 during ramped heating to 1000 °C under 62 – 83% steam. Figure and caption adapted from [1].

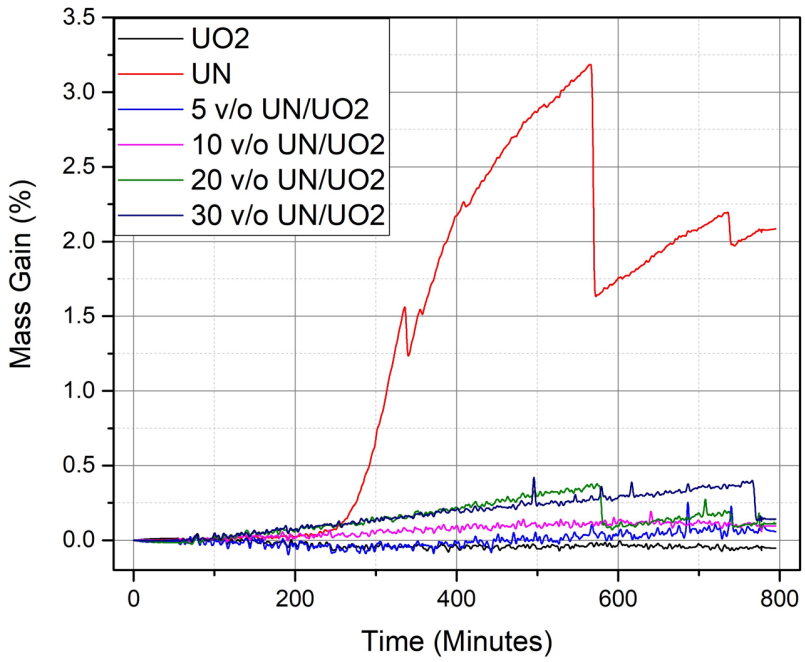

Figure 2: Isotherm data for monolithic UO_2, UN, and four composite materials collected at 350 °C under 82% steam for 12-hr. Figure and caption adapted from [1].

From the UN-UO_2 compositing effort, three concepts to control the microstructure of uranium mononitride to prevent oxidation were: (1) sintering with a more electropositive metal (with a protective oxide) to act as a sacrificial anode during the corrosion reaction (i.e. cermet) , (2) sintering with a ceramic that is highly resistant to corrosion that will act to protect the fuel as a whole (co-sintering), and (3) coating pellets with a corrosion-resistant material, either metal or ceramic.

Work in FY19 focused on ceramic-metal (cermet) composites and one ceramic-ceramic (cercer) composite. To that end, previous work in FY19 examined the feasibility of cermets with more electropositive metals, such as zirconium and yttrium, with the hope that these metals would behave as sacrificial anodes during corrosion of the fuel pellet. However, it was found that more electropositive metals also tended to absorb nitrogen from the uranium mononitride, resulting in composites of uranium mononitride, uranium metal, and other metal nitrides. This is highlighted in Figure 3, which plots an Ellingham diagram for the formation of nitrides. Figure 3 shows that metals such as yttrium, zirconium, titanium, and aluminum all have Gibb's energies of nitride formation that are lower than that of uranium mononitride, indicating that these elements all have higher affinities for nitrogen that does uranium metal. Due to this, these metals will react with nitrogen from UN to form the respective metal nitrides. Conversely, iron, chromium, and silicon have lower affinities for nitrogen, indicating that these metals will remain metallic when interacting with uranium mononitride.

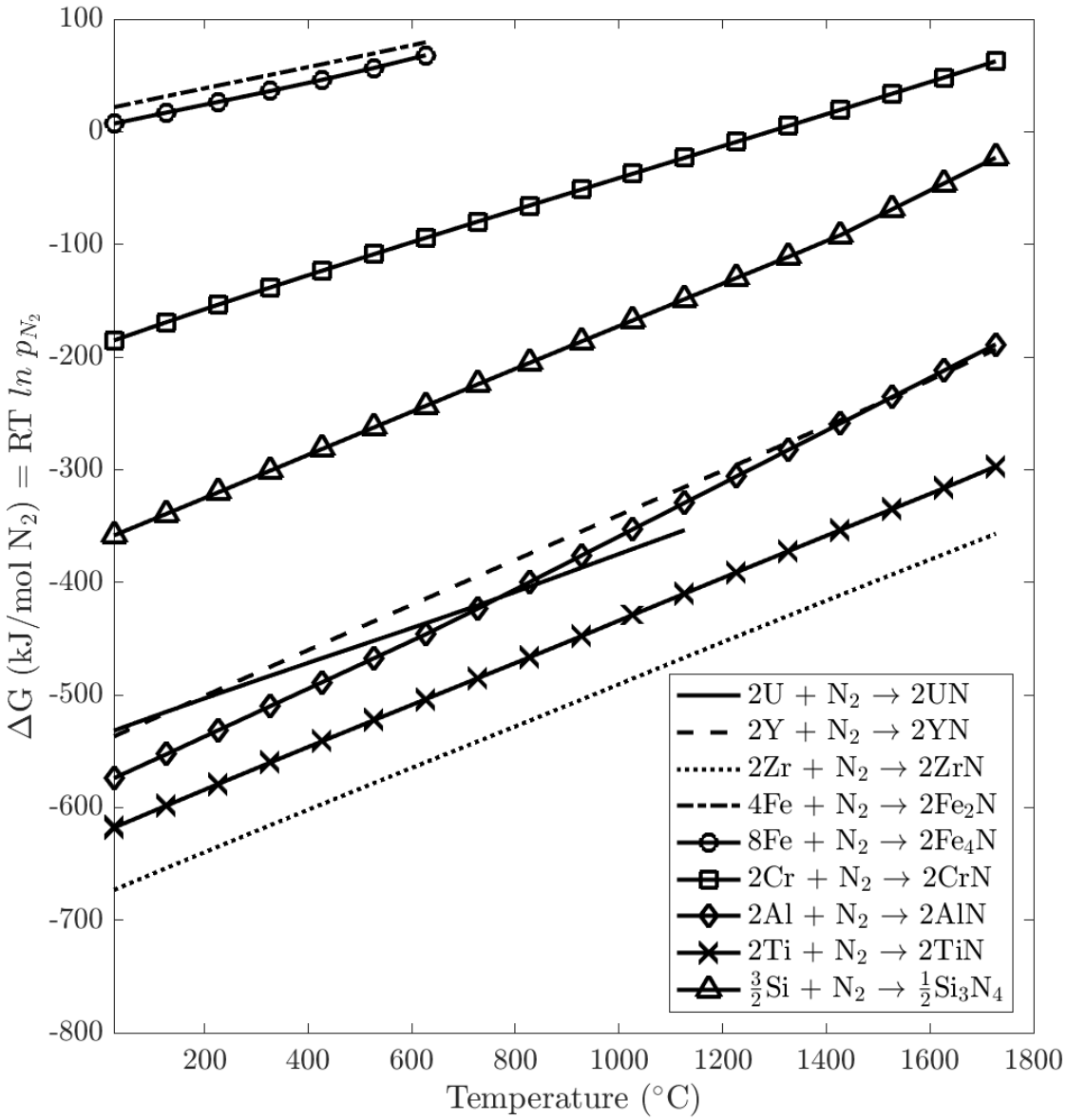

Figure 3: Ellingham diagram for nitriding of various candidate materials for developing microstructurally-engineered uranium mononitride.

From the previous FY19 work highlighted above, the focus of this L2 milestone shifted to cermet concepts with less electropositive metals that exhibited corrosion resistance. This corrosion resistance was evaluated through steam oxidation screening studies of candidate materials. In particular, the scope of this work was focused on silicon (Si) and chromium (Cr), as well as tests of the feasibility of silicon carbide (SiC) as a cercer composite. Focus was also paid to reactive sintering of SiC using graphite and silicon powders. This was done to examine the feasibility of pressing composite pellets of UN, Si, and graphite powders and reactively-sintering to form UN-SiC composites. X-ray diffraction (XRD) was used to determine the final phase composition. As mentioned above, to supplement the sintering study, steam oxidation tests were

conducted on candidate waterproofing materials materials to elucidate candidate material systems that would enhance the corrosion resistance of UN assuming a composite microstructure could be fabricated. Thermodynamic evaluations were also conducted to assess the compatibility of these composite fuel designs coupled with experiments to validate the modeling efforts. Discussion of the results focusses on the feasibility of UN cermet concepts using the aforementioned additives along with additional proposed cercer concepts for future efforts towards corrosion resistance of UN.

2. EXPERIMENTAL METHODS

2.1 Steam corrosion screening studies

Materials for steam corrosion testing were chosen based on oxidation resistance and the protective nature of the oxides. Candidate materials included high-purity silicon and chromium metal that were commercially procured. Silicon (Cerac 99.999% pure) and chromium (Alfa Aesar Puratronic, 99.997% metals basis)) metal pieces were used for steam oxidation testing.

A simultaneous thermal analyzer (STA 449 F3, Netzsch Instruments, Selb, Germany) with a water vapor furnace and water vapor generator (DV2ML, Astream, Germany) was used to perform steam corrosion tests and measure mass change as a function of exposure time *in situ* at various temperatures. Samples were placed in an alumina crucible to contain pulverized pellets during exposure and sample temperature was monitored using a type-S thermocouple. An image of the steam corrosion setup is shown in Figure 4. Results were compared with those of materials examined previously [2].

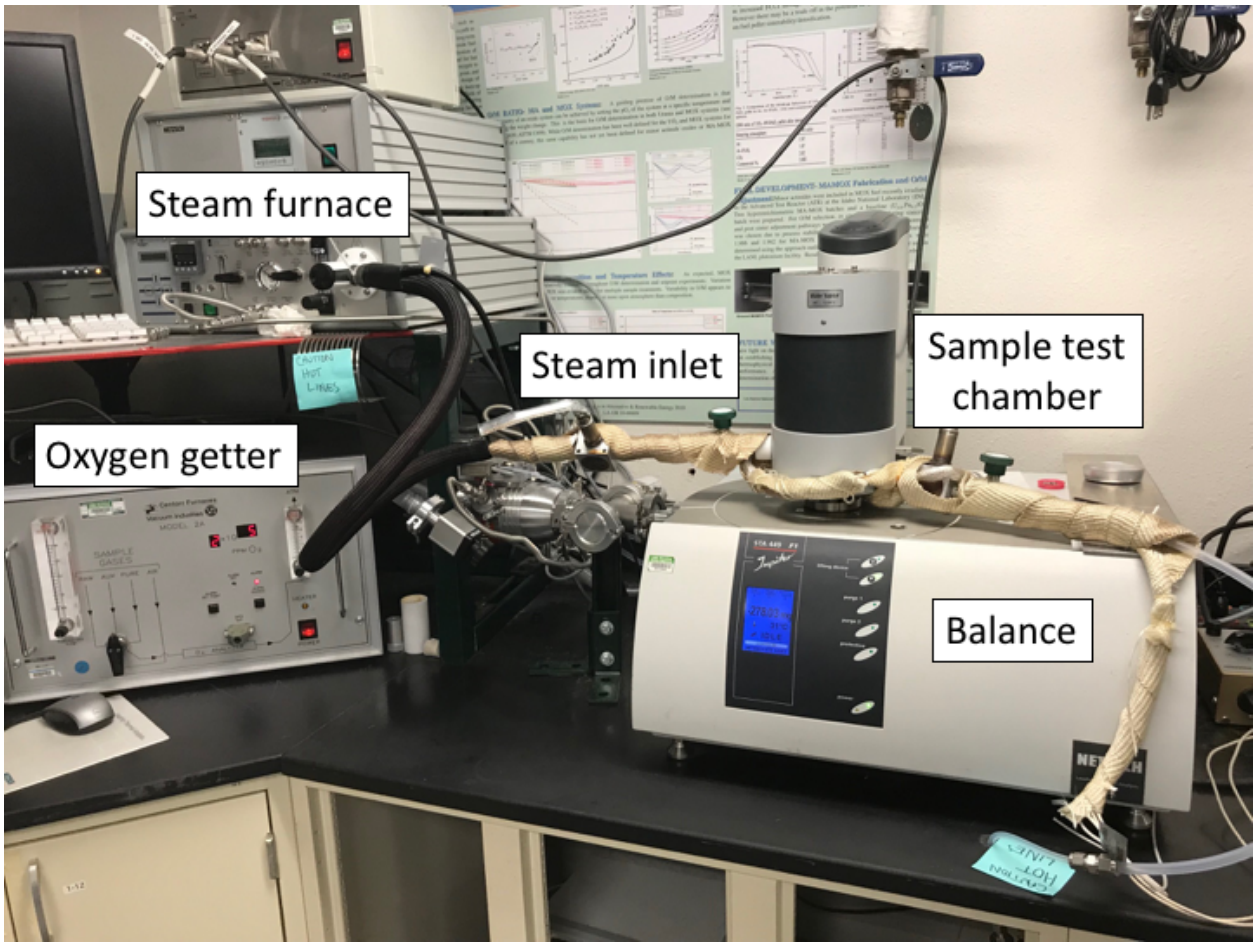

Figure 4: Experimental setup for steam TGA analysis. Annotations indicate major components of the system.

Samples were ramped up to 200 °C in gettered argon at 10 °C/min and allowed to stabilize for 30-min before introduction of steam. Temperature was increased from 200 °C to 1000 °C at 10 °C/min. Once the sample had achieved the maximum temperature, the steam was turned off and the sample was cooled in

gettered argon to room temperature. For all tests, the water vapor flowrate was maintained at 9.14 g/hr of water. Gettered argon at 8 L/hr (calibrated with nitrogen) acted as a carrier gas for the steam, while a protective gas of gettered argon at 20 mL/min was purged through the balance during each run. This resulted in a steam content ranging from 75% at 200 °C to 89% at 1000 °C.

2.2 Uranium mononitride composite fabrication

Starting material used for this study was received from Areva (Courbevoie, France) as hyperstoichiometric uranium(IV) oxide, which was reduced to stoichiometric $UO_{2.00}$ under reducing conditions and converted to UN using the carbothermic reduction to nitridation process. As mentioned above, silicon, chromium, and silicon carbide materials commercially procured.

Uranium mononitride and respective metal powders were separately size-reduced and sieved through a -325 mesh sieve (44-μm). The appropriate amounts of uranium mononitride and respective metal powder were then co-milled for 5-minutes with 0.25 wt. % ethylene bis(stearamide) (EBS) binder to mix the two materials. Theoretical densities were calculated using the rule of mixtures based on volume. Composite pellets were pressed at 150 MPa using a 5.2-mm punch and die set and then sintered at specific temperatures based on the melting point of the respective metal in gettered argon in a W-mesh furnace. All material processing in this study was performed in an inert, argon glovebox with oxygen and water contents maintained below 50 and 0.1 ppm, respectively. A simultaneous thermal analyzer (STA 449 F3, Netzsch Instruments, Selb, Germany) with a tungsten furnace was also used to perform sintering studies and measure mass change *in situ* as a function of exposure time and temperature. Pellets were placed on a UN setter plate for sintering to prevent reaction with crucible and furnace materials.

Composite samples of UN-M were fabricated with theoretical compositions as given in Table 1, where M represents the additive material: silicon, chromium, or silicon carbide. Silicon material was the same as for steam STA testing; chromium powder was procured from Exotech with an average particle size of approximately 44 μm (-325 mesh), while the average particle size of the silicon carbide powder was approximately 50 μm (-240 mesh). Additionally, one silicon-graphite pellet was pressed to examine reactive sintering of silicon carbide as a potential pathway for producing UN-SiC composites. The graphite used to produce this pellet was procured from Alfa Aesar and was pure to 99.9995% metals basis. The silicon-graphite pellet was pressed with 70:30 silicon-to-graphite molar ratio to account for potential volatilization of silicon. This ratio was chosen based on literature work studying reactive sintering of silicon carbide [3].

Table 1: Summary of cermet and cercer compositions considered in this study. Table also shows the theoretical densities and sintering temperatures for the respective waterproofing concept.

Additive -	Volume fraction of additive (%)	Theoretical density (g/cm^3)	Sintering temperature(s) (°C)
Si	40	9.53	1500
Cr	40	11.48	2000, 1800, 1700
SiC	40	9.88	2100, 2050

2.3 Phase purity analysis

XRD was used to analyze the phase content of the composites with uranium mononitride. A Bruker XRD (D2 Phaser, Bruker AXS, Madison, WI, USA) was used for these analyses. XRD scans were performed with 2θ ranging between 10 and 90° with a 0.01° 2θ-step and a 7-s acquisition time for each step. Material for all XRD examinations were homogenized using a mortar and pestle in an inert, argon glovebox and encapsulated in a low-background XRD sample holder to prevent exposure to air.

3. RESULTS AND DISCUSSION

3.1 Steam corrosion testing of candidate materials

Samples of silicon and chromium metal were subjected to steam oxidation during temperature ramps to 1000 °C to determine the protective nature of the oxide layer that formed. Results were compared with those of cast yttrium, silicon carbide, and APMT (Fe-Cr-Al alloy) that were performed for the related L3 milestone [2]. Comparison was also drawn with an archive steam oxidation test of sponge zirconium, due to the ubiquitous nature of zirconium-based alloys in light water reactors and the well-characterized corrosion performance of these alloys. Results of the temperature ramp oxidation tests are given in Figure 5, which plots the extent of oxidation as a function of temperature. The extent of oxidation is defined as unity when all components of the material have oxidized and assumes no formation of hydroxides or spinel phases. That is, chromium oxidized to chromium(III) oxide (Cr_2O_3) and silicon oxidized to silicon(IV) oxide (SiO_2). As a result, the y-axis in Figure 5 is a reaction coordinate quantifying the extent of the oxidation reaction.

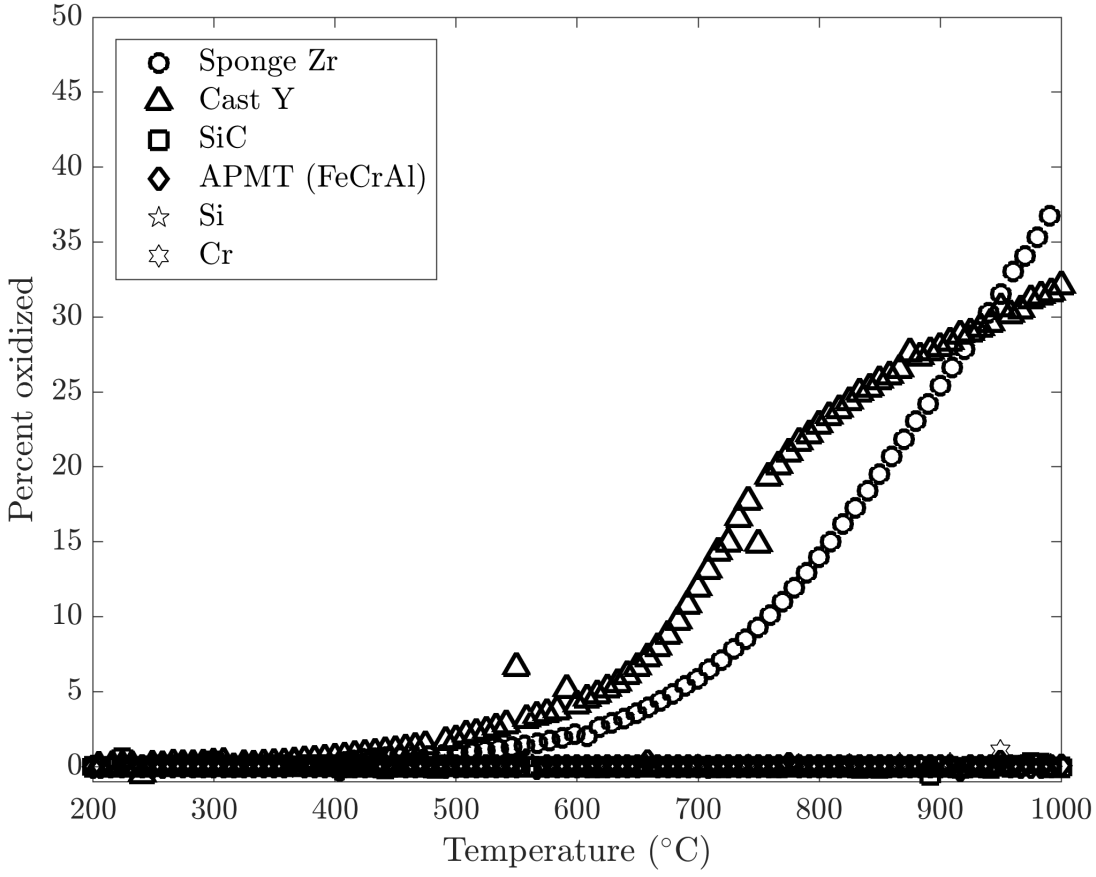

Figure 5: Thermograms comparing degree of oxidation (in percent oxidized) as a function of temperature for silicon and chromium during ramped heating to 1000 °C under 75% to 89% steam atmosphere. Results were referenced to those obtained for sponge Zr (archive), cast Y, SiC, APMT from the related L3 milestone [2].

Figure 5 shows that, of the metals and alloys tested, yttrium and sponge zirconium were the least resistant to corrosion, while APMT, silicon carbide, silicon, and chromium all exhibited little to no oxidation within

the detection limit of the STA balance. As highlighted in the previous milestone, it was hypothesized that the yttrium and zirconium oxide layers were protective at low temperature, but not so at higher temperatures [2]. As a result of the oxidation resistance demonstrated during these tests, it was determined that the focus of this L2 milestone would be the compositing of uranium mononitride with silicon, chromium, and silicon carbide. Fe-Cr-Al alloys were not selected for compositing due to the thought that, once melted, the beneficial microstructure of these alloys that afford good mechanical properties and resistance to oxidation would no longer be present.

3.2 Synthesis of UN composites

3.2.1 UN-Cr cermets

Composites of uranium mononitride and chromium were sintered at 2000, 1800, and 1700 °C, which are above, or close to, the melting point (1857 °C) of chromium. The sintering profiles attempted in an STA are shown in Figure 6, which plots mass change and sample temperature as a function of time in gettered argon.

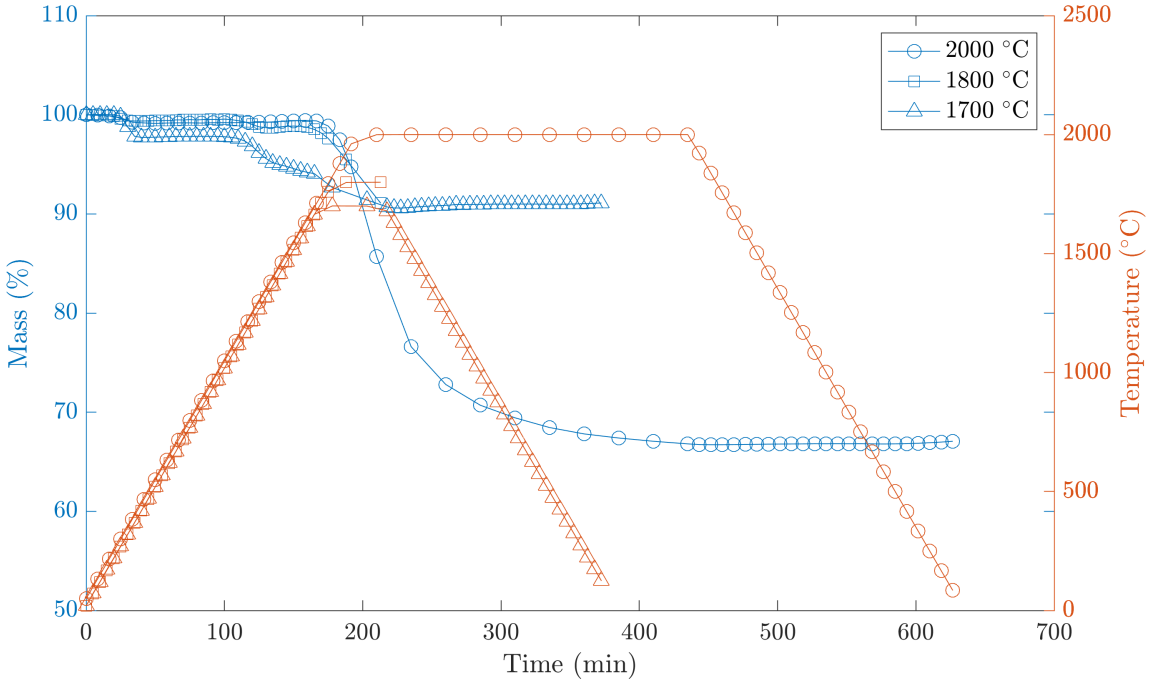

Figure 6: Sintering profiles for the synthesis of UN-Cr cermets. Sample mass is plotted in blue, while sample temperature is plotted in orange. The line markers indicate the temperatures associated with the mass change and temperature profiles. The data for 1800 °C overlaps with the data for 2000 °C up to approximately 200 minutes, then overlaps with the data for 1700 °C.

Figure 6 shows significant mass loss during sintering at 2000 °C. This mass loss was tempered by reducing the sintering temperature. However, decreasing sintering to 1800 and 1700 °C is anticipated to result in conventional sintering rather than liquid-phase sintering given the melting point of chromium.

A summary of pellet compositions and final densities are summarized in Table 2. Samples exhibited much lower density than expected and showed significant mass loss. As was the case with UN-Si composites, comparison with theoretical density was not feasible due to inability to measure initial pellet masses (fragile pellets) and the significant mass loss during liquid-phase sintering. An example pellet of UN-40Cr is shown

in Figure 7, which shows a black layer around the pellet. It was hypothesized that this black layer was due to the presence of an oxide. This was confirmed using XRD, which also showed only a small amount of chromium. An example XRD pattern is given in Figure 8.

Table 2: Summary of the chromium contents and sintered densities for UN-Cr cermets. Sample #1 was not able to be measured for final dimensions/mass because it fused to the sample crucible and was unable to be retrieved.

Sample –	Initial volume percent Cr (%)	Sintering temperature (°C)	Final mass (g)	Anticipated Cr mass loss (g)	Sintered density (g/cm^3)
1	43.2	2000	-	-	-
2	38.1	1800	0.49325	0.055	8.10
3	38.8	1700	0.4918	0.055	5.02

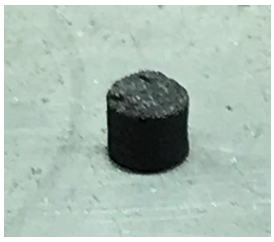

Figure 7: Image of UN-40Cr pellet after attempted sintering in the W STA. The pellet shows signs of oxidation based on the presence of the black layer on the pellet surface.

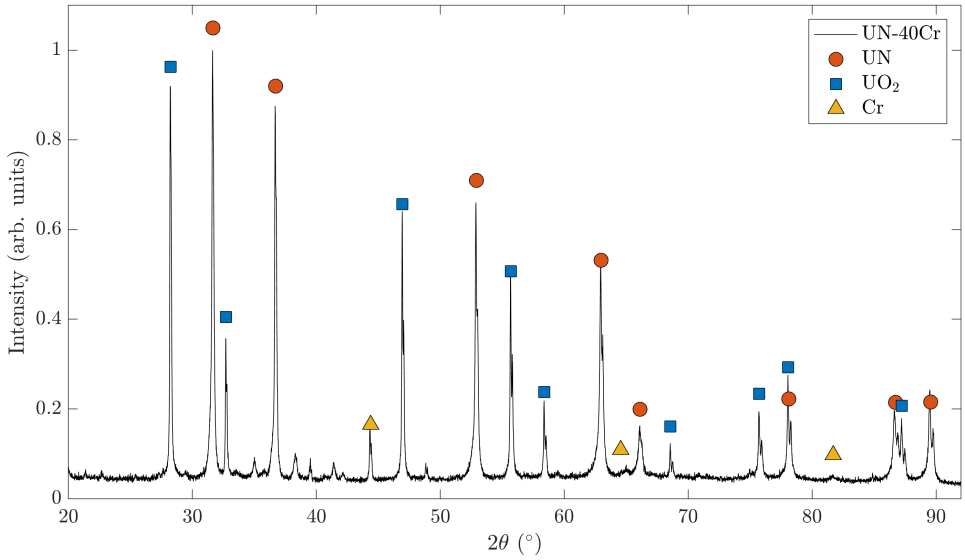

Figure 8: Representative XRD pattern for the UN-40Cr pellet sintered at 1800 °C. Results indicated that little Cr remained due to volatilization.

From Figure 8, some chromium was observed, though the predominant phases identified were uranium mononitride and uranium(IV) oxide. As with the UN-Si cermets, it is believed that the uranium(IV) oxide was formed during transfer of the green pellet from the inert, argon glovebox to the benchtop tungsten STA.

The results presented here indicate the importance of vapor pressure for the waterproofing concepts. From the Sloan chart of density and vapor pressure of common elements, the vapor pressure of chromium is 1 torr (0.0013 atm) at 1504 °C. Extrapolation of the known vapor pressure data to the sintering temperatures in this study revealed that the expected partial pressure of chromium was 2.25 torr (0.0030 atm) at 1700 °C, 3.24 torr (0.0043 atm at 1800 °C, and 4.95 torr (0.0065 atm) at 2000 °C. Due to the fact that sintering was performed under flowing argon, the equilibrium chromium vapor pressure was not maintained. Thus, chromium was slowly removed from the system to try to maintain an equilibrium pressure of chromium. For future efforts examining metals with higher vapor pressures, it may be necessary to use static systems under which equilibrium conditions may be maintained.

3.2.2 UN-Si cermets

Composites of uranium mononitride and silicon were sintered at temperatures above the melting point of silicon, approximately 1410 °C. Liquid-phase sintering was performed at 1500 °C in gettered argon. An example sintering profile is shown in Figure 9, which plots mass change and sample temperature as functions of time.

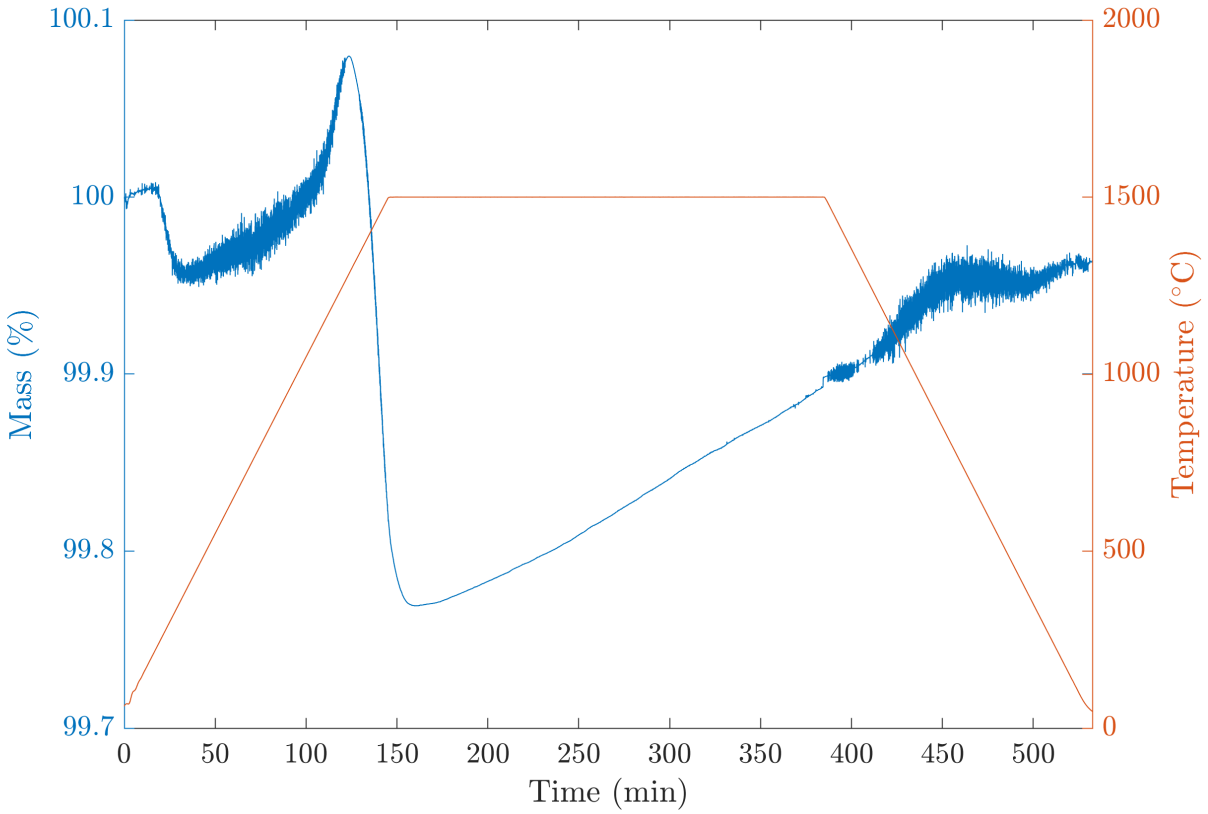

Figure 9: Example sintering profile for the synthesis of UN-Si composites. Sample mass is plotted in blue, while sample temperature is plotted in orange.

Figure 9 shows some mass loss at temperature followed by slow mass gain. It is hypothesized that the mass loss corresponded to the denitriding of uranium, while the slow mass gain was due to slight oxidation of the composite. The Sloan vapor pressure chart for common elements showed that the vapor pressure of silicon near 1600 °C is approximately 0.1 torr (0.00013 atm), which was not expected to result in significant

volatilization. This emphasizes the idea that mass loss for UN-Si composites was due to denitriding of uranium mononitride.

A summary of pellet compositions and final densities are summarized in Table 3. Samples exhibited much lower density than expected, but remained robust and difficult to pulverize. A comparison with theoretical density was not feasible due to inability to measure initial pellet masses (fragile pellets) and mass loss during liquid-phase sintering. To answer why this was the case, samples were examined for phase content using XRD. An example resultant UN-40Si pellet is shown in Figure 10, while a representative XRD pattern for a UN-40Si pellet is shown in Figure 11.

Table 3: Summary of the silicon contents and sintered densities for UN-40Si cermets.

Sample –	Initial volume percent Si (%)	Sintered density (g/cm^3)
1	35.7	5.92
2	40.3	5.92
3	40.3	5.83
4	40.3	5.95

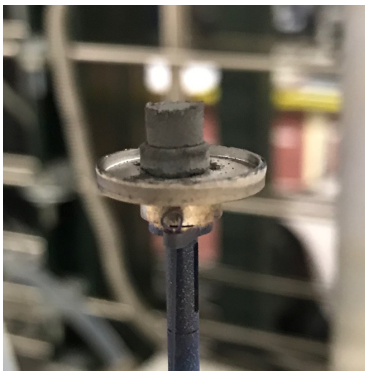

Figure 10: Image of UN-40Si pellet after attempted sintering in the W STA. The UN-40Si pellet is located on top of a UN setter plate to prevent reaction between the silicon and the crucible material.

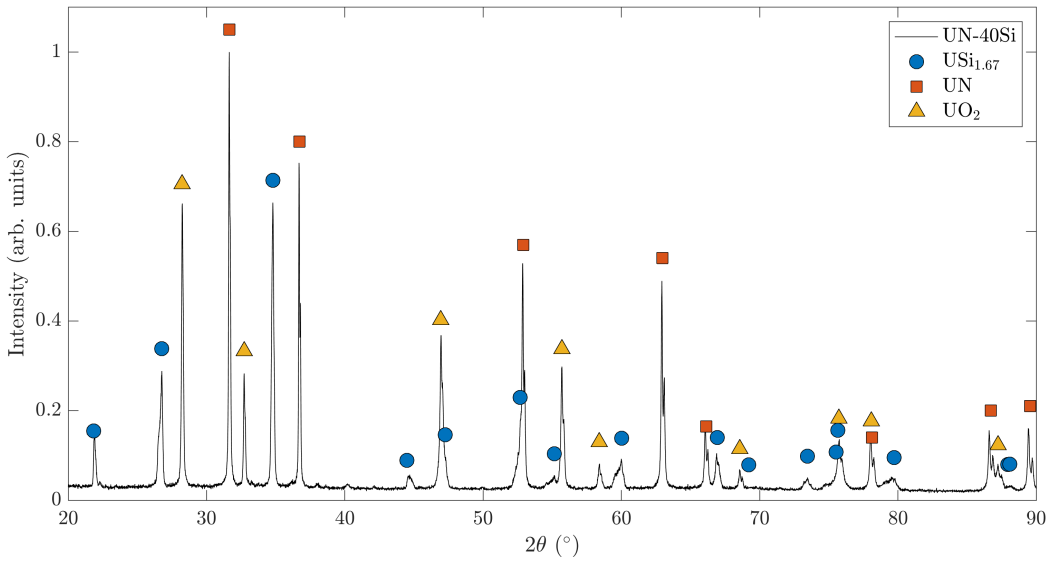

Figure 11: Representative XRD pattern for a UN-40Si pellet. Results indicated that the Si reacted with UN to form $USi_{1.67}$.

From Figure 11, no silicon was observed within the detection limits of the XRD detector. However, uranium silicides were detected, indicating that the liquid silicon reacted with the uranium mononitride/de-nitrided uranium to form small amounts of uranium silicides. It is assumed that this reaction proceeded to completion, as no other silicon-bearing phases were observed. Uranium(IV) oxide was also observed. Because the sintering was performed in a benchtop tungsten furnace, it is believed that some oxidation occurred during transfer of the green pellet from the inert, argon glovebox to the benchtop instrument, as well as during the sintering measurement.

To understand the formation of silicides from uranium mononitride, the thermodynamics of silicide and nitride formation were assessed using ThermoCalc 2019a (Thermo-Calc Software AB, Solna, Sweden) and the SGTE Substances Database 6.0. The compounds considered for the calculations included: UN, U_3Si, U_3Si_2, USi_2, USi_3, and U_3Si_5. Gibbs free energy was calculated for the reactions and were normalized to the moles of uranium participating in the reaction. Figure 12 plots the Gibbs free energy of formation for these compounds as a function of temperature.

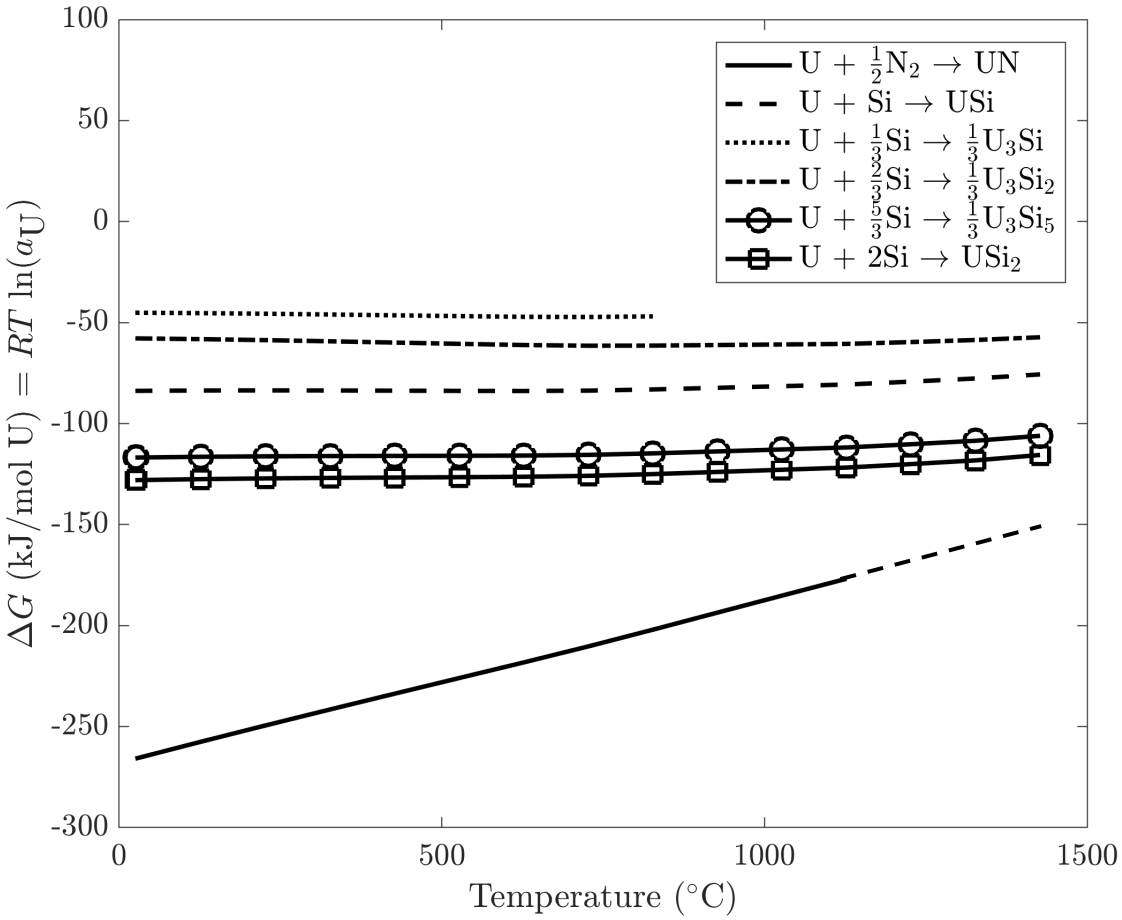

Figure 12: Gibb's free energy as a function of temperature for the formation of UN and uranium silicides. The U-UN line terminated at 1127 °C, which is close to the melting point of uranium metal. The dashed line continuing the U-UN formation energy calculation is extrapolation to beyond the melting point of uranium.

From Figure 12, it is observed that uranium mononitride is much more stable than are the silicides, especially at temperatures below 1000 °C. This is given by the much more negative Gibb's free energy of formation, indicating greater spontaneity of the forward-proceeding reaction. However, extrapolation of the curve for uranium mononitride formation shows that, at increased temperature, it approaches the lines for several uranium silicide compounds and appears to cross these lines at temperatures exceeding 1800 °C. The thermodynamics of this system is being investigated further by other groups, as well [4]. It should be noted that data for uranium mononitride formation was not available in the SGTE Substances 6.0 database. As a result, it is difficult to draw conclusions for temperatures close to 1500 °C, the temperature at which liquid-phase sintering was attempted. Complications in the reactions could arise from desorption of nitrogen from uranium mononitride, as well as the melting of silicon. These are not fully captured in this plot, as data to higher temperatures would be required.

3.2.3 UN-SiC composite system

As mentioned above, the feasibility of synthesizing composites of uranium mononitride and silicon carbide was evaluated using two different methodologies. The first was through the reactive sintering of silicon and

graphite powders above the melting point of silicon, while the second was through the pressing and sintering of a UN-SiC composite pellet. The purpose of these studies was to show (1) the feasibility of liquid-phase sintering to produce UN-SiC composites and (2) demonstrate the direct sintering of uranium mononitride with silicon carbide.

3.2.3.1 Liquid-phase sintering of silicon-carbide

Pellets of silicon and graphite were sintered in the W STA using a UN setter plate to prevent reaction between the silicon and the tungsten crucible. Figure 13 shows a schematic of the experimental setup.

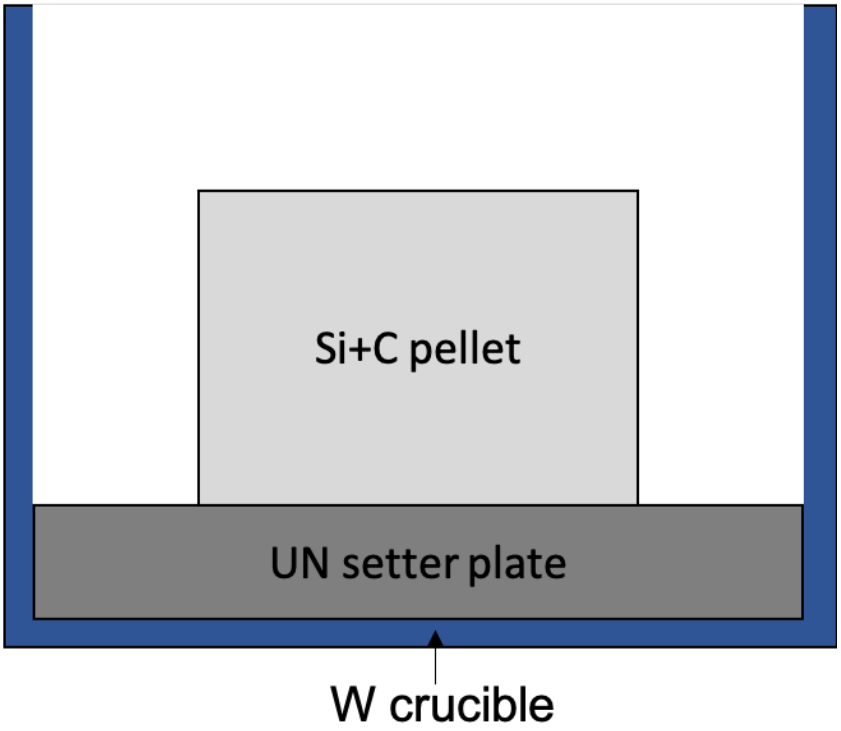

Figure 13: Schematic of setup for liquid-phase sintering of SiC from silicon and graphite powders. A UN setter plate was used to prevent reactions between liquid silicon and the W crucible.

As mentioned before, the silicon-graphite pellet consisted of a 70:30 molar ratio of silicon to carbon to account for potential volatilization of silicon. The initial mass of the pellet consisted of 0.870 g of silicon and 0.156 g of graphite, resulting in an experimental molar ratio of 71:29 for silicon to carbon. The sintering profile used to study reactive sintering is shown in Figure 14.

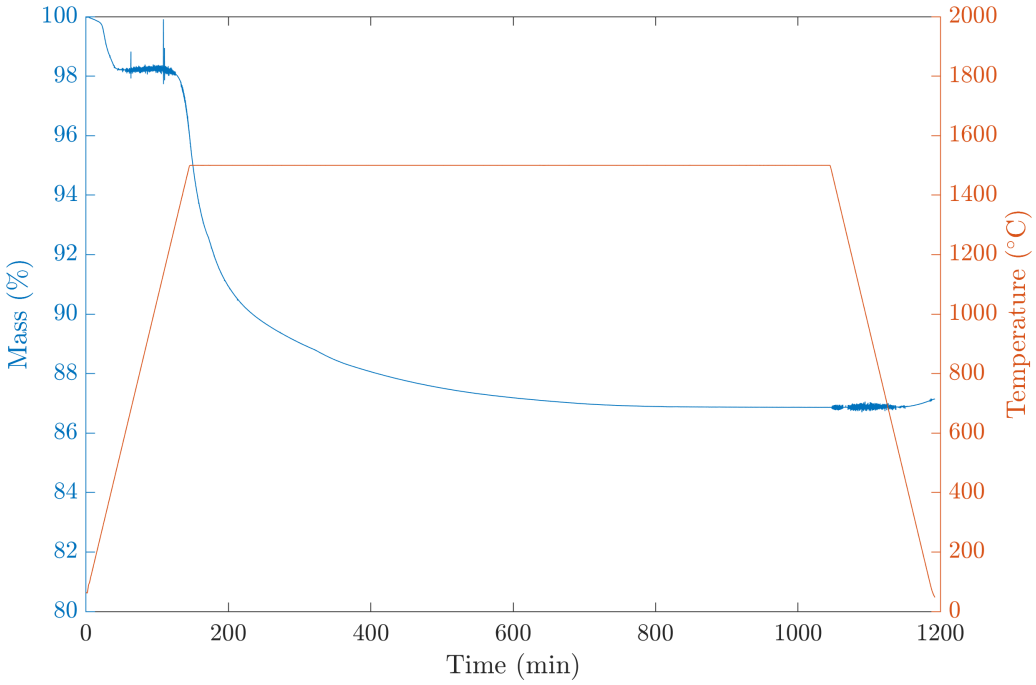

Figure 14: Sintering profile for the reactive sintering of silicon and graphite to form silicon carbide. Sample mass is plotted in blue, while sample temperature is plotted in orange.

Figure 14 shows mass loss during sintering at 1500 °C. As with the UN-Si composites, the mass loss was attributed to denitriding of the uranium mononitride setter plate. An image of the final silicon/graphite pellet is shown in Figure 15. The resultant pellet was heavily cracked and had reacted with the UN setter plate, which is shown in Figure 16.

Figure 15: Image of silicon-graphite pellet after reactive sintering. Pellet was heavily cracked and pulverized upon handling.

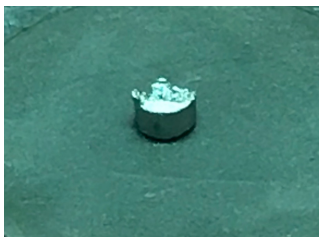

Figure 16: Image of UN setter plate after silicon-graphite reactive sintering.

To explain the interaction between the silicon, graphite, and UN, XRD was performed on both the cracked silicon-graphite pellet and the UN setter plate. The XRD pattern obtained from the silicon-graphite pellet is shown in Figure 17, while the pattern obtained from the UN setter plate is shown in Figure 18.

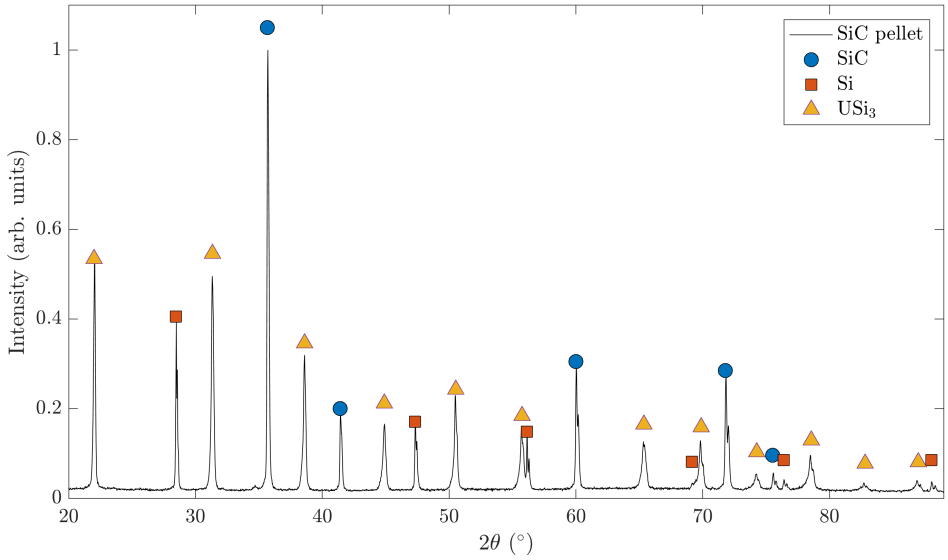

Figure 17: Representative XRD pattern for the silicon/graphite pellet sintered at 1500 °C. Results indicated that the pellet was predominantly SiC with some free silicon. Some of the silicon had additionally reacted with the UN setter plate to form USi_3, which interacted with the silicon/graphite pellet.

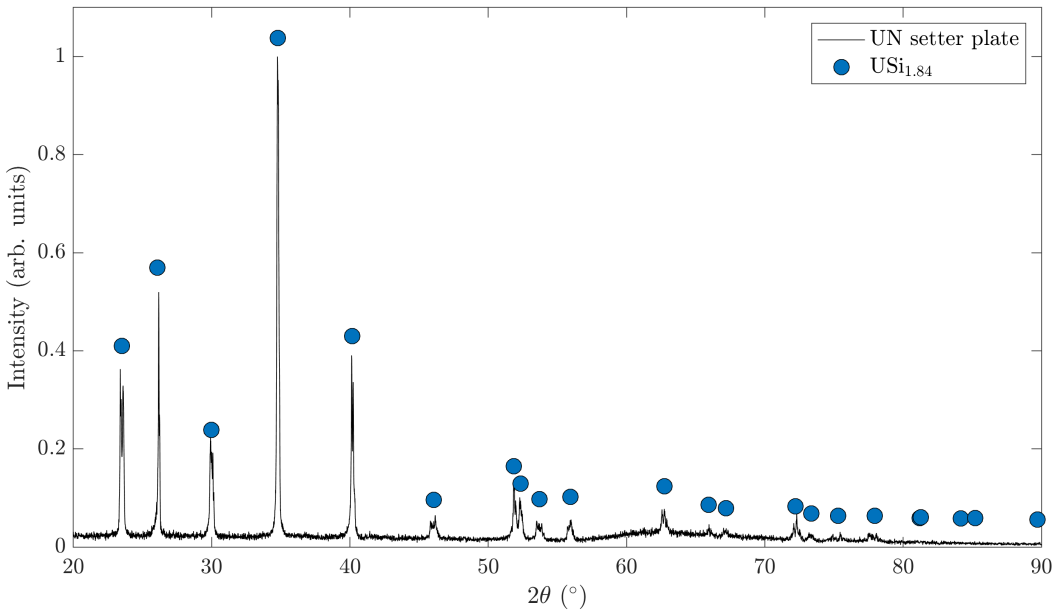

Figure 18: XRD pattern obtained from the UN setter plate used for SiC reactive sintering. Results indicate that the silicon from the Si/C pellet reacted with the setter plate to form a uranium silicide, $USi_{1.84}$.

From Figure 17, the principal phase observed was silicon carbide, indicating that the reactive sintering was a partial success, though some free silicon was also detected. However, the presence of uranium silicides in the silicon/graphite pellet indicated that some of the silicon had reacted with the uranium mononitride setter plate. This was further corroborated from the XRD of the setter plate in Figure 18, which shows nearly complete conversion from uranium mononitride to a uranium silicide phase, with no detectable amount of uranium mononitride.

To determine whether the use of silicon carbide for waterproofing uranium mononitride was still a viable option, one composite pellet of uranium mononitride and silicon carbide was pressed with 0.153 g of silicon carbide and 0.660 g of uranium mononitride, resulting in a volume percent of 50.9% silicon carbide, which was slightly higher than desired. This pellet was sintered, using two-step sintering, as has been done in the literature for pressure-less sintering of silicon carbide. The sintering involved a short high-temperature step at 2100 °C and a subsequent long step at 2050 °C. This is shown in Figure 19.

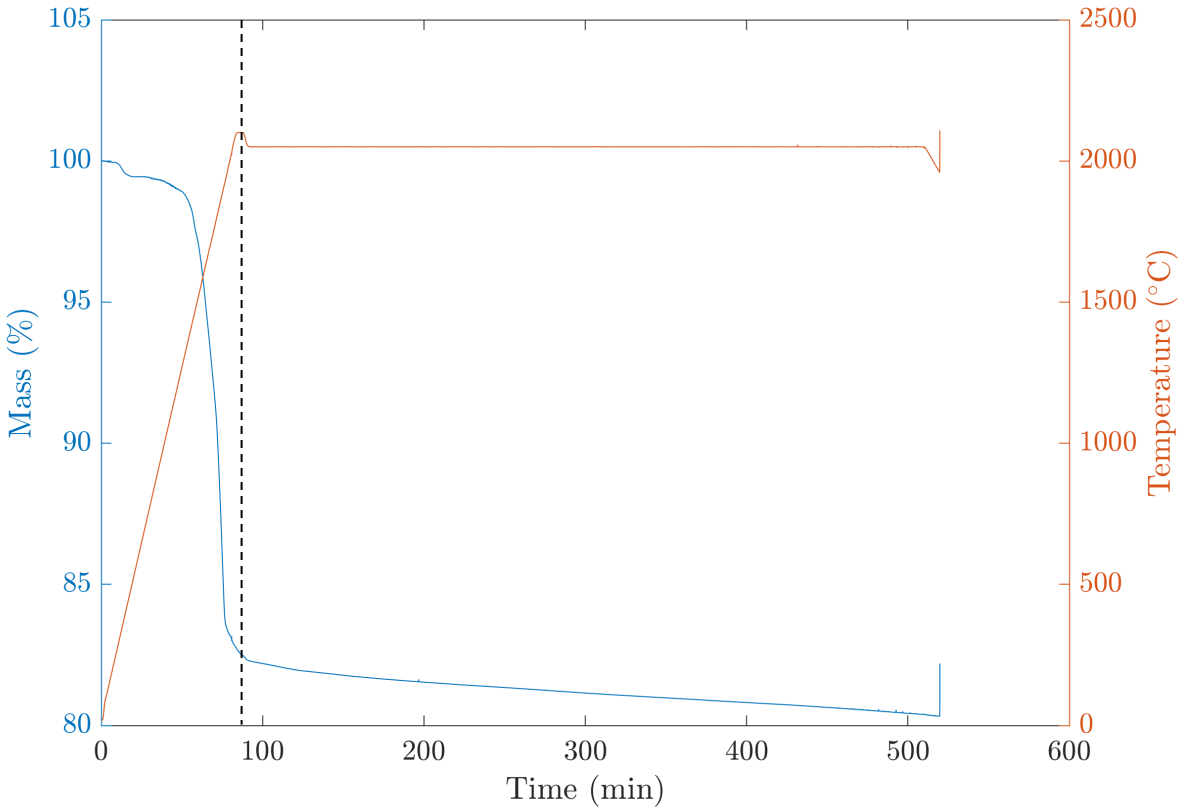

Figure 19: Sintering profile for the two-step sintering of UN and silicon carbide. The dashed line demarcates the two steps in the sintering procedure. Sample mass is plotted in blue, while sample temperature is plotted in orange. Mass and temperature signals were lost at approximately 520 min due to a sudden break of the thermocouple wire.

Figure 19 shows significant mass loss at temperatures in excess of approximately 1500 °C. This is highlighted in Figure 20, which plots mass, in percent, as a function of temperature. As silicon carbide is stable to such temperatures, it is hypothesized that the mass loss occurred due to chemical interaction between denitrided uranium and the silicon carbide. Examination of the sample and crucible after the attempted sintering run showed significant interaction with the tungsten crucible with little of the pellet or crucible remaining. Due to the importance of the UN-SiC system for applications aside from waterproofing

uranium mononitride for LWR applications, the chemical interactions and thermodynamics of this system are being explored further.

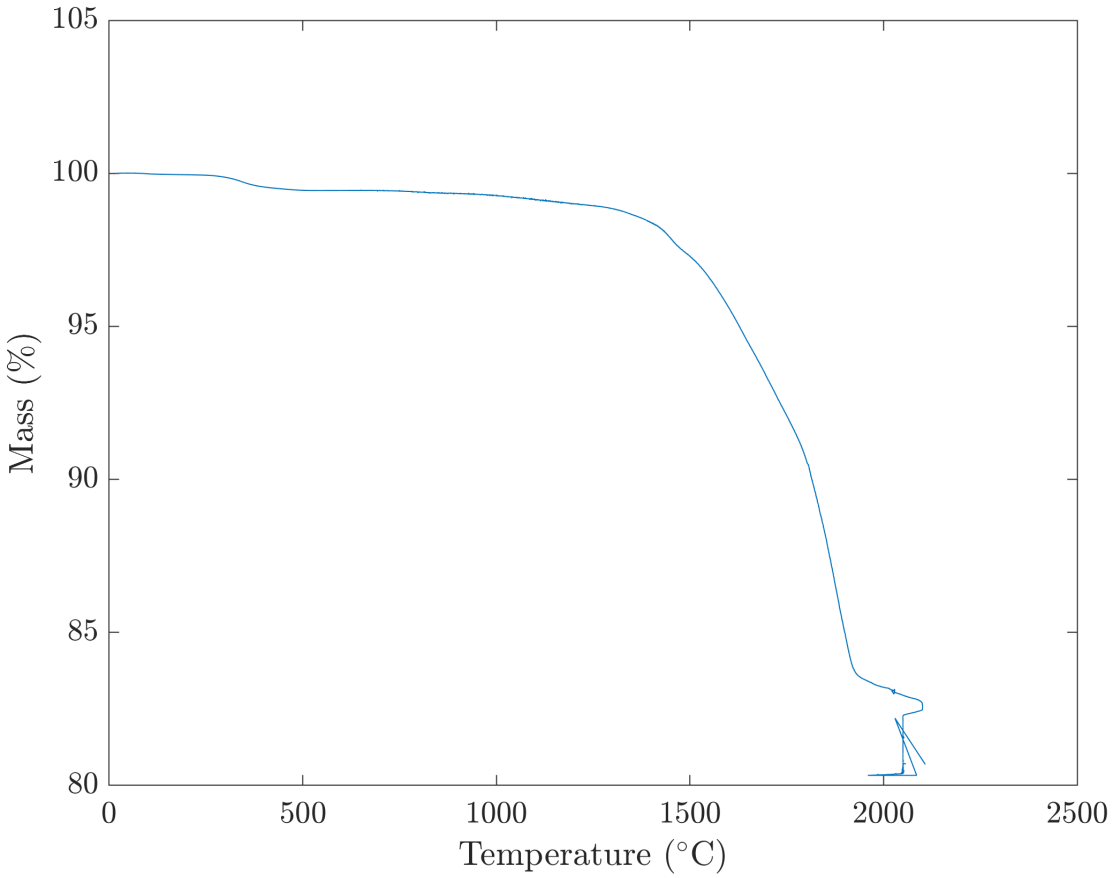

Figure 20: Mass as a function of temperature for UN-SiC direct sintering. Significant mass loss is apparent starting near 1500 °C.

As was done for the UN-Si system, thermodynamic calculations were performed to plot the Gibb's free energy of formation for the relevant silicon-containing compounds including: SiC, USi, U_3Si, U_3Si_2, USi_2, USi_3, and U_3Si_5. Gibb's free energy was normalized to the moles of silicon and plotted as a function of temperature, as shown in Figure 21.

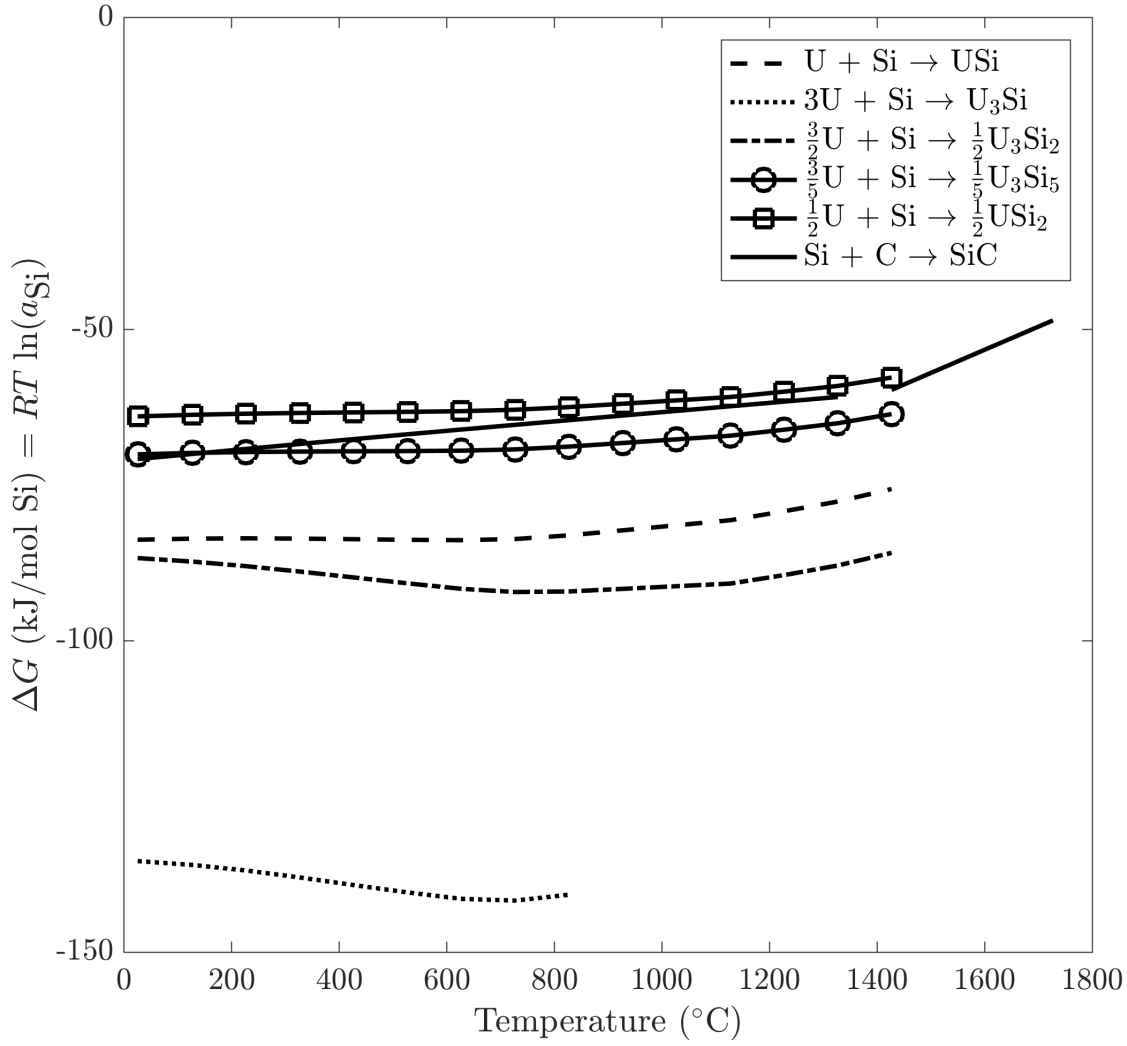

Figure 21: Gibb's free energy of formation for silicon-containing compounds relevant to UN-SiC sintering.

From Figure 21, it is observed that on the basis of moles of silicon, silicon carbide is less thermodynamically stable than many of the uranium silicides and its stability decreases with increasing temperature, as shown by the more positive slope in Gibb's energy as a function of temperature as compared with the silicides. As a result, the current hypothesis regarding what occurred during the sintering attempt is that the silicon carbide and uranium mononitride reacted to form a uranium silicide compound and free silicon. Although uranium nitride by itself is more stable than many of the uranium silicides, the addition of silicon carbide would have increased the system Gibb's free energy. One way to reduce the system Gibb's free energy could have been the formation of silicides. Based on the uranium-silicon binary phase diagram, the uranium silicide with the highest melting point is U_3Si_5, which has a melting point of approximately 1770 °C [5]. At temperatures above this, it is clear that any uranium silicides would be liquid and could have reacted with the tungsten crucible used to hold the pellet. An attempt was made to identify the remaining uranium-containing compound left on the sample thermocouple. However, because the sample fused to the tungsten crucible and the tungsten-rhenium thermocouple, it was difficult to identify the uranium-containing

compounds. Some materials that the XRD software interpreted included uranium dicarbide (UC_2) and various uranium silicides. Due to the complexity of the system for sintering UN-SiC pellets, more work to understand the chemical interactions between uranium mononitride and silicon carbide at temperature are warranted. This is especially important given that interactions with crucible materials may have played a role in causing sample loss/melt.

3.3 Thermodynamic considerations for UN waterproofing

From the results of this L2 milestone, as well as the L3 milestone that preceded it, waterproofing efforts focused on uranium mononitride will need to be re-evaluated. Particularly with regards to reactivity between the fuel and waterproofing materials. In the preceding L3 milestone it was found that liquid-phase sintering with metals more electropositive than uranium led to the reaction with nitrogen to form uranium metal and other metal nitrides [2]. The results of this L2 highlight the importance of understanding reactivity between uranium and the waterproofing material. Silicon and silicon carbide were both found to react with uranium mononitride to form silicides. Volatility was also found to be an important issue, as chromium was found to volatilize in some capacity at temperature and denitriding of uranium mononitride was also hypothesized to be an issue.

To that end, the thermodynamics that need to be considered for waterproofing of uranium mononitride include evaluations of resistance to waterside corrosion and to chemical interaction between the fuel matrix and the waterproofing compound. This was done above for the UN-Si system for the case of silicide formation, as well as evaluating the thermodynamic stability of silicon carbide with respect to uranium silicides. In the prior sections it was found that silicon carbide is less thermodynamically stable than the uranium silicides. This instability increased with temperature and may have driven the formation of uranium silicides to reduce the overall Gibb's free energy of the system.

An example of a similar analysis is presented here for another waterproofing concept: co-sintering of uranium mononitride with aluminum mononitride. As with the UN-Si system, the properties of interest include the propensity to gain/lose nitrogen to uranium, the ability of aluminum to react with uranium, and the resistance to corrosion. From Figure 3, it is observed that aluminum mononitride is thermodynamically more stable at temperatures below 800 °C, but less stable at higher temperatures. This could involve losing nitrogen to uranium at higher temperatures. The assessment of the thermodynamic stability of several uranium-containing compounds, including uranium aluminides, is shown in Figure 22.

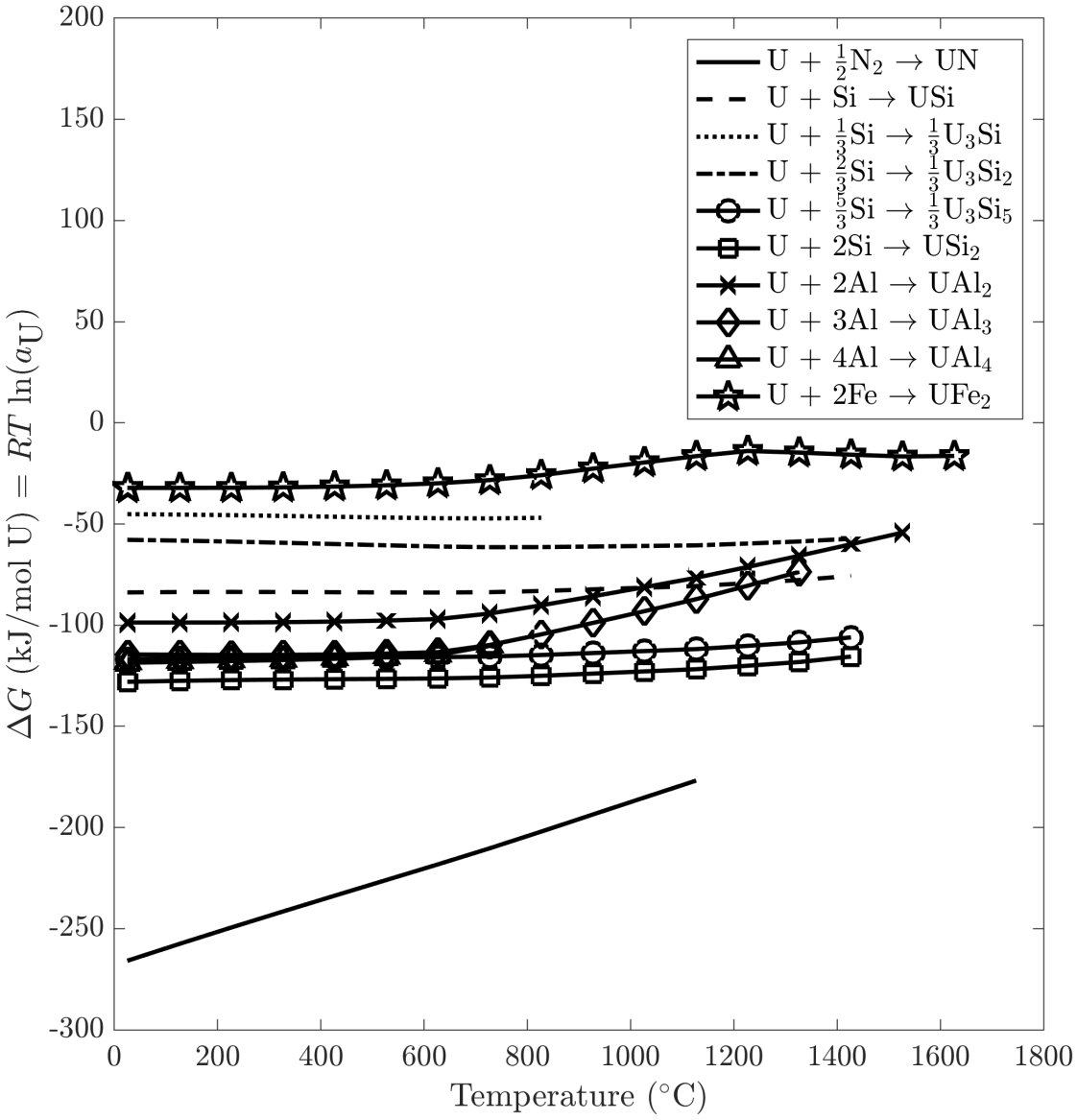

Figure 22: Gibb's free energy as a function of temperature for the formation of uranium intermetallics and compounds relevant to UN waterproofing concepts.

From Figure 22, it is observed that the uranium aluminides are less stable than uranium mononitride and have similar stabilities to the silicides. However, the thermodynamic stability of aluminum mononitride must also be compared with respect to those of the aluminides to determine whether the aluminum in aluminum mononitride might react with uranium to form aluminides. Gibb's free energy as a function of temperature for the relevant aluminum-containing compounds is plotted in Figure 23.

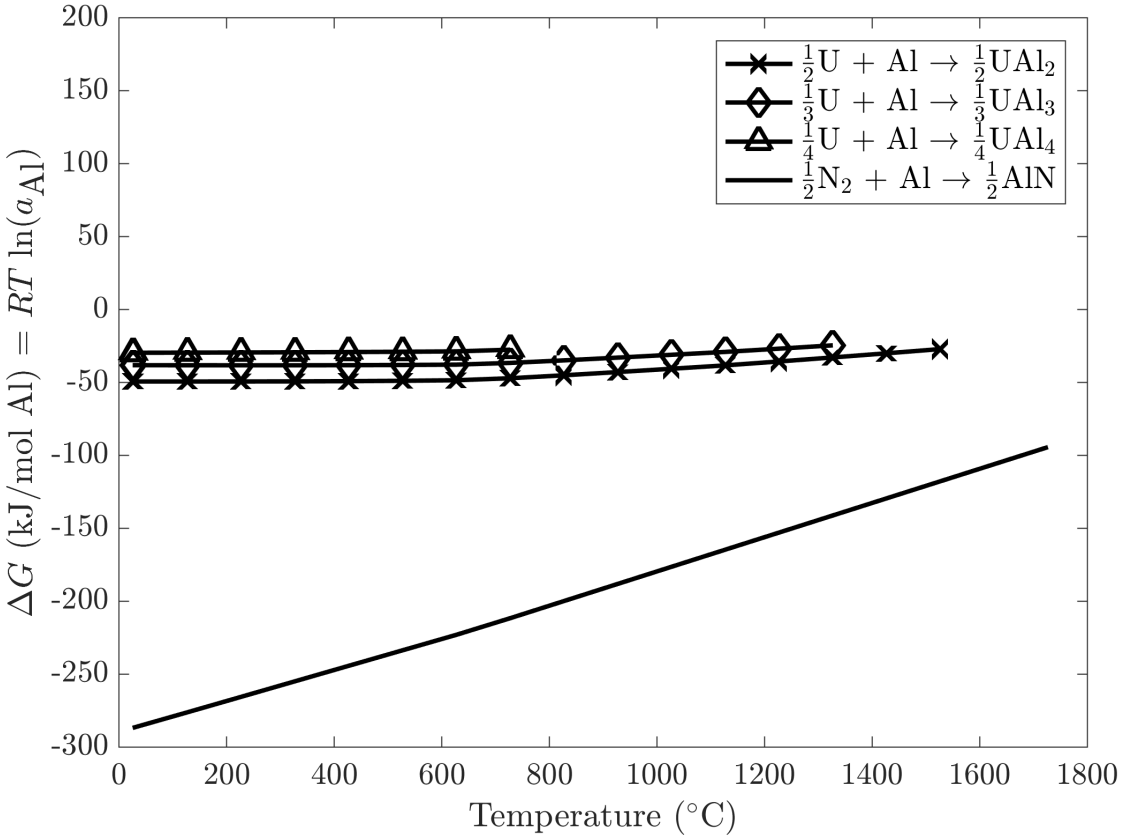

Figure 23: Gibb's free energy as a function of temperature for aluminum-containing compounds relevant to the UN-AlN waterproofing concept.

From Figure 23, it is observed that aluminum mononitride is more stable than the uranium aluminides on the basis of moles of aluminum. However, it can be seen that the Gibb's energy as a function of temperature for aluminum mononitride has a higher slope than do those for the uranium aluminides. Thus, it is expected that higher temperatures might result in the formation of the aluminides from uranium mononitride and aluminum mononitride. It should be noted that these plots do not account for de-nitriding of aluminum, which would result in the formation of aluminum metal, which would then melt at temperatures above 660 °C.

As was for chromium, vapor pressure of aluminum could be an issue, especially if nitrogen desorbs from aluminum mononitride. Aluminum mononitride is typically sintered using hot pressing, but can be sintered by pressure-less sintering at temperatures between 1600 and 2000 °C [6]. The vapor pressure of aluminum at 1749 °C is approximately 100 torr (0.132 atm) and at 2327 °C is 1 atm. While it is unlikely that aluminum should form from aluminum mononitride, the complex chemistry highlighted above between uranium mononitride and aluminum mononitride necessitate the consideration of aluminum volatilization under the conditions required to sinter composites of these materials.

Finally, the resistance of aluminum to waterside corrosion with respect to uranium must be considered. An Ellingham diagram for oxidation in water vapor of uranium mononitride, aluminum mononitride, and various metals relevant to waterproofing efforts is shown in Figure 24.

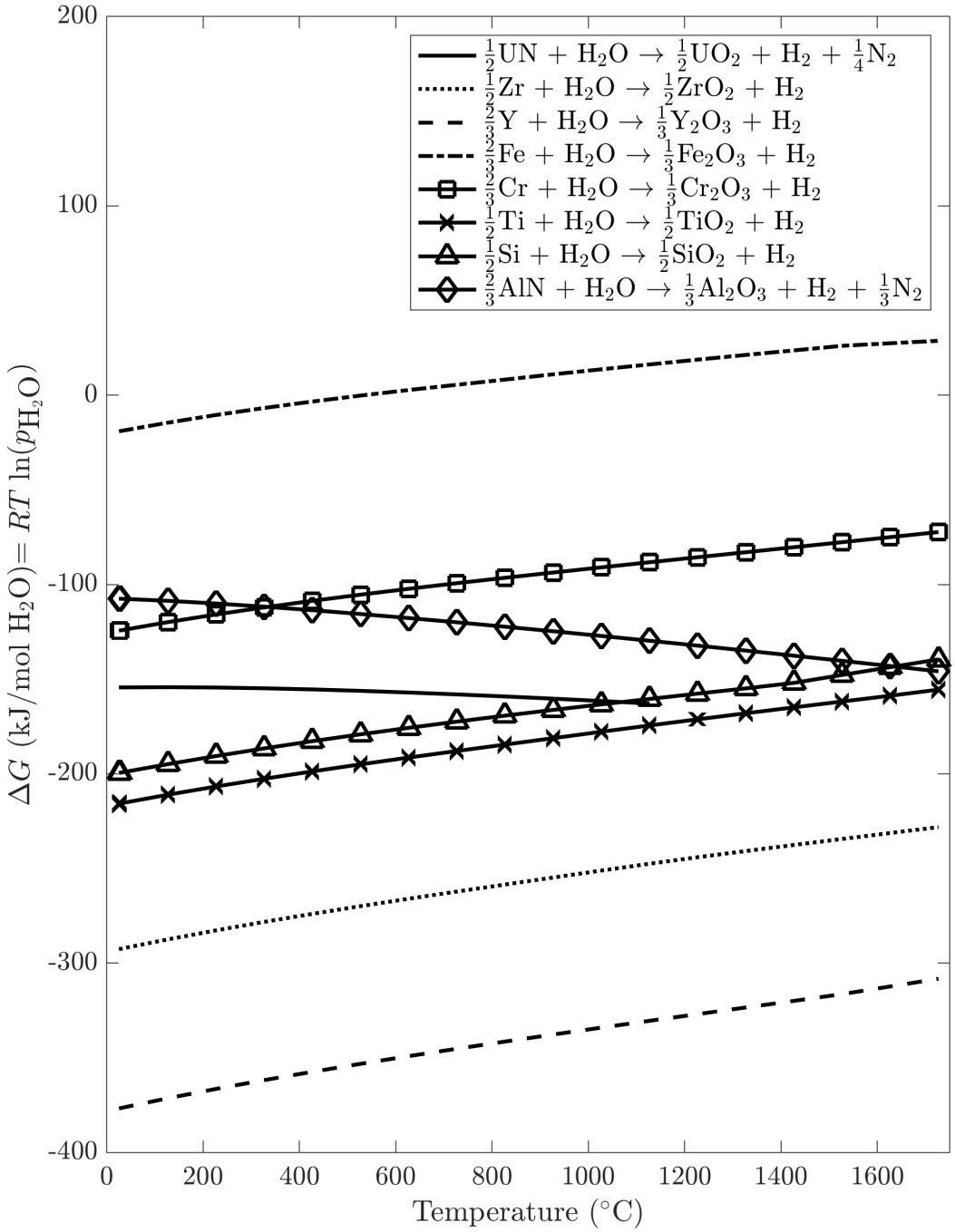

Figure 24: Ellingham diagram for the formation of oxides by water vapor corrosion. Curves shown for uranium mononitride, aluminum mononitride, and various metals/metalloids relevant to waterproofing efforts. Attention is called to uranium mononitride (solid line) and aluminum mononitride (solid line with diamond markers).

From Figure 24, it is observed that aluminum mononitride (solid line with diamonds) is less likely to oxidize under waterside corrosion conditions than is uranium mononitride (solid line). As a result, under these conditions, uranium mononitride will preferentially oxidize. This means that aluminum mononitride will not sufficiently protect uranium mononitride from waterside corrosion unless it can protect the individual grains or is applied as a coating. As a co-sintered composite, aluminum mononitride will not preferentially oxidize and will not contribute to waterproofing. It is also important to examine the formation of hydroxide phases, as this was not considered in this analysis and these hydroxides may form during waterside corrosion.

While this type of analysis has not been performed for all of the various waterproofing concepts being considered, it does show the thermodynamics that must be considered moving forward to understand material interactions. The analysis presented above for aluminum mononitride showed that, at high temperatures, composites with uranium mononitride have the ability to form aluminides, which may be more stable than aluminum mononitride at very high temperature, especially with chemical interactions with uranium mononitride. Additionally, de-sorption of nitrogen from aluminum mononitride could result in the formation of free aluminum. At the sintering temperatures considered for composite synthesis, aluminum would have a very high vapor pressure, resulting in the volatilization of significant amounts of free aluminum. Finally, aluminum mononitride was shown to be less likely to oxidize under waterside corrosion conditions, indicating that it would not be able to sufficiently protect uranium mononitride from oxidation unless applied as a coating or if coating the individual uranium mononitride grains.

Moving forward with waterproofing efforts, the ideal material with which to synthesize composites, such as cermets and cercers, with uranium mononitride would have little chemical interaction with uranium beyond basic solubility (no intermetallic or stoichiometric compounds), would have a low vapor pressure at sintering temperatures, would not preferentially absorb nitrogen from uranium, would preferentially oxidize with respect to uranium, and would exhibit protective oxidation behavior under waterside corrosion conditions. Coating options would require many of the same properties with the exception that the material need not oxidize preferentially with respect to uranium.

4. CONCLUSIONS AND FUTURE WORK

In an effort to waterproof uranium mononitride, several different approaches were considered, including liquid-phase sintering with oxidation-resistant metals, co-sintering with oxidation-resistant ceramics, and coating. This L2 milestone focused on liquid-phase sintering with silicon and chromium metals, as well as co-sintering with silicon carbide. The steam-oxidation resistances of these materials were simultaneously examined and compared with those of other materials tested in the prior L3 milestone. Results indicated that silicon, chromium, and silicon carbide might be promising candidate materials due to their resistance to oxidation in steam as compared with zirconium, which is traditionally used in-reactor. Materials in powder form were mixed with uranium mononitride powder in specific compositions, pressed, and heated to respective temperatures for sintering: liquid-phase sintering in the cases of silicon and chromium, and two-step sintering in the case of silicon carbide. However, attempts to sinter uranium mononitride with these materials resulted in un-anticipated interactions, as observed from XRD and thermogravimetry. In the cases of silicon and silicon carbide, reactions with uranium mononitride resulted in the formation of uranium silicides, while in the case of chromium, the high vapor pressure of chromium at sintering temperatures and the dynamic system resulted in loss of chromium over time.

These observations suggest that silicon and chromium are not suitable for liquid-phase sintering with uranium mononitride and silicon carbide is not suitable for co-sintering with this material. To determine a path forward for waterproofing efforts, thermodynamic calculations were performed with the aim of understanding the interactions that need to be understood before qualifying a waterproofing concept. An example analysis was performed for aluminum mononitride as a cercer concept. The thermodynamics indicated that co-sintering with aluminum mononitride may result in the formation of uranium aluminides and that aluminum mononitride would not preferentially oxidize with respect to uranium mononitride. As a result, aluminum mononitride would not sufficiently waterproof uranium mononitride as a cercer concept, though it could work as a coating concept. Future concepts should be evaluated on the basis of reactivity with uranium (should not form stoichiometric compounds), reactivity with nitrogen (should not absorb nitrogen from uranium), vapor pressure (should not significantly volatilize), and resistance to waterside corrosion (should form a protective oxide layer over a wide temperature range). Finally, cermet and cercer concepts should also preferentially oxidize with respect to uranium mononitride so as to prevent fuel pulverization.

Future efforts on waterproofing studies of uranium mononitride will holistically examine steam oxidation resistance and resistance to reaction with uranium mononitride, as within the scope outlined above. As waterproofing concepts and candidates are identified and evaluated, the matrix of samples to test in steam using TGA will continue to expand.

5. REFERENCES

[1] N. R. Wozniak and J. T. White, "Determination of the feasibility to waterproof UN for LWR use." 27-Jul-2018.

[2] A. P. (ORCID:0000000185152756) Shivprasad, C. J. Grote, and J. T. (ORCID:0000000244092264) White, "Development of and initial assessment of microstructurally engineered UN," Los Alamos National Lab. (LANL), Los Alamos, NM (United States), LA-UR-19-22533, Jul. 2019.

[3] G. G. Gnesin and A. I. Raichenko, "Kinetics of the liquid-phase reactive sintering of silicon carbide," *Powder Metall Met Ceram*, vol. 12, no. 5, pp. 383–389, May 1973.

[4] D. A. Lopes *et al.*, "Experimental and computational assessment of USiN ternary phases," *Journal of Nuclear Materials*, vol. 516, pp. 194–201, Apr. 2019.

[5] H. Vaugoyeau, L. Lombard, and J. P. Morlevat, "Contribution a l'etude du diagramme d'equilibre uranium silicium," *Journal of Nuclear Materials*, vol. 39, no. 3, pp. 323–329, Jun. 1971.

[6] K. Komeya and H. Inoue, "Sintering of Aluminium Nitride," *Journal of the Ceramic Association, Japan*, vol. 77, no. 884, pp. 136–143, 1969.